Synthesis, Structural Characterizations, and Some Chemical Properties of a Fibrous Titanate with a Novel Layer/Tunnel Intergrown Structure

Takayoshi Sasaki,* Mamoru Watanabe, Yoshinori Fujiki, and Yoshizo Kitami

National Institute for Research in Inorganic Materials, 1-1 Namiki, Tsukuba, Ibaraki 305, Japan

Received March 24, 1994. Revised Manuscript Received June 8, 1994[⊗]

A fibrous alkali titanate with a novel layer/tunnel intergrown structure, $M_{6+\delta}Ti_{16}O_{35+\delta/2}$ (M = K, Rb; $-0.7 < \delta < +0.5$), has been prepared from a protonic layered tetratitanate $H_2Ti_4O_9 \cdot 1.2H_2O$ through a soft chemical route: adjustment of the interlayer alkali/proton composition by ion-exchange and subsequent dehydration around 350 °C. X-ray and electron diffraction data as well as a (010) high-resolution lattice image for the typical composition of $\delta = 0$ have demonstrated that the titanate crystallizes in a primitive monoclinic system with the unit cell parameters $a \sim 17$ Å, $b \sim 3.8$ Å, $c \sim 12$ Å, and $\beta \sim 97°$. The host framework is built up from two structural elements, the tetratitanate-type layer unit of $Ti_8O_{18}^{4-}$ and the octatitanate-type tunnel one of $Ti_8O_{17}^{2-}$, which are stacked in a nearly alternating way along the a axis. Half of the alkali metal ions are accommodated in the layer part and the other half are in the tunnel. This hybrid structure is consistent with the suggestion by Tournoux et al. (*Prog. Solid State Chem.* **1986**, *17*, 33). The interlayer cations are reactive, participating in reversible hydration and ion-exchange, while the tunnel ones are inert. The hybrid compound was unstable at elevated temperatures where it was disproportionated into thermodynamically stable titanates. Mixed valent derivatives, $A_xM_6Ti_{16}O_{35}$ (A = Li, K; $0.5 < x < 1.5$), were obtained by reductive intercalation of K and Li via the action of K metal vapor and n-butyllithium, respectively.

Introduction

During the past decade, a new concept of soft chemistry has attracted considerable attention as a new synthetic approach in the field of solid-state chemistry.[1−5] This kind of synthetic strategy employs low-temperature processes, e.g., ion-exchange, redox intercalation/deintercalation, electrochemical reactions, with the aim of fabricating or even tailoring novel materials, often metastable ones, which are hardly achieved by conventional routes through high-temperature processes.

Among a variety of soft chemical syntheses reported so far, one of the most beautiful examples is the preparation of an octatitanate $K_2Ti_8O_{17}$ with a tunnel structure from a layered tetratitanate $K_2Ti_4O_9$.[3,6−8] The host layers in $K_2Ti_4O_9$ are condensed in a topotactic manner resulting in one-dimensional tunnels in $K_2Ti_8O_{17}$ (see Figure 1). This is induced by half-protonation of the interlayer composition and subsequent dehydration at moderate temperatures of 300−500 °C.

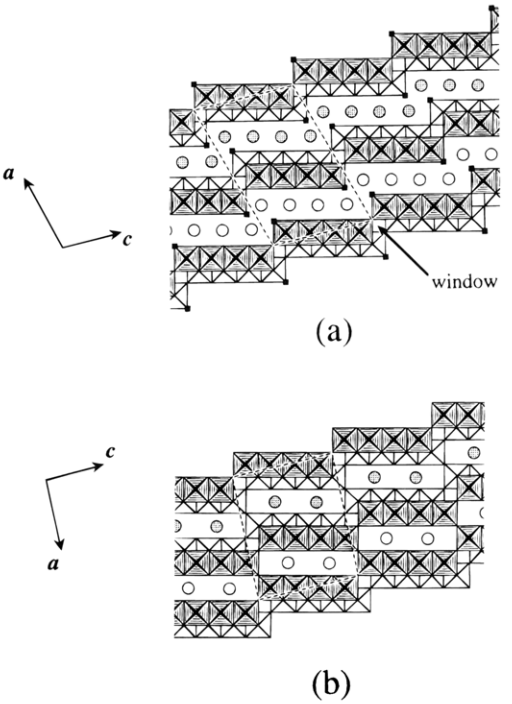

Figure 1. Crystal structure for (a) tetratitanate $M_2Ti_4O_9$ (M = K, Rb)[9,10] and (b) octatitanate $M_2Ti_8O_{17}$[11] viewed down along the b axis. The dashed lines encircle the unit cell. The circles represent K or Rb ions. The hatched octahedra and stippled circles are at the level of $y = 0$. Closed squares in (a) are terminal oxygen atoms which are the most basic in the structure.

[⊗] Abstract published in *Advance ACS Abstracts,* July 15, 1994.

(1) Schöllhorn, R. *Angew. Chem., Int. Ed. Engl.* **1980**, *19*, 983.
(2) Figlarz, M. *Chem. Scr.* **1988**, *28*, 3.
(3) Tournoux, M.; Marchand, R.; Brohan, L. *Prog. Solid State Chem.* **1986**, *17*, 33.
(4) Clearfield, A. *Chem. Rev.* **1988**, *88*, 125.
(5) Papers in *Soft Chemistry Routes to New Materials*; Rouxel, J., Tournoux, M., Brec, R., Eds.; Trans Tech Publications: Aedermannsdorf, 1994.
(6) Marchand, R.; Brohan, L.; Tournoux, M. *Mater. Res. Bull.* **1980**, *15*, 1129.
(7) Marchand, R.; Brohan, L.; M'Bedi, R.; Tournoux, M. *Rev. Chim. Miner.* **1984**, *21*, 476.
(8) Sasaki, T.; Fujiki, Y. *J. Solid State Chem.* **1989**, *83*, 45.
(9) Verbaere, A.; Tournoux, M. *Bull. Soc. Chim. Fr.* **1973**, *4*, 1237.
(10) Dion, M.; Piffard, Y.; Tournoux, M. *J. Inorg. Nucl. Chem.* **1978**, *40*, 917.
(11) Sasaki, T.; Watanabe, M.; Fujiki, Y.; Kitami, Y.; Yokoyama, M. *J. Solid State Chem.* **1991**, *92*, 537.

0897-4756/94/2806-1749$04.50/0

Similar acid–base solid-state syntheses have been reported: A metastable polymorph of TiO_2 with the Freudenbergite-type structure is obtained from layered titanates such as $Na_2Ti_3O_7$, $K_2Ti_4O_9$, and $Cs_2Ti_5O_{11}$.[3,6,7,12–14] A layered titanoniobate $KTiNbO_5$ is converted into a novel substance $Ti_2Nb_2O_9$, characterized by its unusual void tunnels.[15,16]

In connection with the preparation of $K_2Ti_8O_{17}$, Tournoux et al. suggested[3,6,7] that a series of hybrid oxides between $K_2Ti_4O_9$ and $K_2Ti_8O_{17}$ is formed on dehydration of the potassium/proton tetratitanate, $K_xH_{2-x}Ti_4O_9{\cdot}nH_2O$ ($1 < x < 2$), the interlayer cation/proton ratio of which is higher than unity for the octatitanate precursor. Despite its intriguing structure and possible attractive properties, the hybrid titanate has not been fully characterized.

We have prepared a protonic tetratitanate $H_2Ti_4O_9{\cdot}1.2H_2O$ in a fibrous form and studied its acid–base properties.[17–20] It has been demonstrated that the exchangeable protons are consumed in four steps evolving four kinds of discrete cation-loaded phases $M_xH_{2-x}Ti_4O_9{\cdot}nH_2O$ where $x = 0.5$, 1.0, 1.5, and 2.0 and M denotes alkali metals. The fibrous K– and Rb–octatitanates were obtained by dehydrating the half cation-loaded tetratitanate ($x = 1.0$)[8] and their structural features were examined, especially focusing on ordered/disordered distribution of the cations in the wide tunnel.[11,21] In continuation of such studies, dehydration of the alkali/proton tetratitanate of loading level $1.0 < x < 2.0$ is reexamined to get a deeper understanding of the layer/tunnel hybrid titanate. The structural characterizations and some chemical properties as well as the synthetic process are described in the present paper.

Experimental Section

Reagents and Materials. All the reagents were of 99.9% purity or higher and used without further purification.

Fibrous crystals of potassium tetratitanate $K_2Ti_4O_9$ were grown from a flux melt of K_2MoO_4 containing K_2O and TiO_2 according to the procedures described previously.[22] The protonic form $H_2Ti_4O_9{\cdot}1.2H_2O$ was obtained from $K_2Ti_4O_9$ by extracting interlayer K ions with aqueous HCl solutions.[17] The titration of $H_2Ti_4O_9{\cdot}1.2H_2O$ with K and Rb ions was carried out by equilibrating it batchwise with a mixed solution of corresponding chloride and hydroxide under similar conditions described elsewhere.[17,20] The ionic strength of the titrant was 0.1 and the ratio of the titrant/protonic titanate was 100 $cm^3\ g^{-1}$.

Characterizations. Powder X-ray diffraction (XRD) data were acquired using a Rigaku RAD-2B diffractometer with graphite-monochromatized Cu Kα radiation ($\lambda = 1.5405$ Å). The unit-cell dimensions were refined by the least-squares method.[23] Electron diffraction patterns and high-resolution lattice images were taken on a JEM-2000EX electron microscope equipped with a double-tilting goniometer (±25°). An Akashi ISI-DS120 scanning electron microscope was used to observe microscopic textures. A Rigaku TAS-200 thermal analyzer was employed to study thermal stability of the hybrid titanate. The diffuse reflectance UV–vis spectra were recorded using a Hitachi U-3500 type spectrophotometer.

Chemical Reduction. The K incorporation was carried out by treating the hybrid titanate (~1 g) with K metal vapor at 280 °C in a vacuum-sealed glass tube. After the treatment, the sample was washed with ethanol and dried in vacuo. Then the product was analyzed by the wet method[8] to determine the amount of K inserted.

The Li intercalation was conducted in an Ar-filled drybox by immersing a weighed amount of the material (0.1 g) in a n-C_4H_9Li/n-hexane solution (10 cm^3, 5×10^{-3}–5×10^{-2} mol dm^{-3}) at ambient temperature. After 5 days, an aliquot of the equilibrated solution was pipetted and its Li content was determined by atomic absorption spectroscopy (Hitachi 180-80 spectrophotometer) after being extracted into a HCl solution. The Li uptake was deduced from a difference between starting and residual concentrations.

Table 1. K- and Rb-Loaded Tetratitanate Obtained by Titration[a]

loading	K	d_{200} (Å)	Rb	d_{200} (Å)
0	$H_2Ti_4O_9{\cdot}1.2H_2O$	9.1	$H_2Ti_4O_9{\cdot}1.2H_2O$	9.1
1/4	$K_{0.5}H_{1.5}Ti_4O_9{\cdot}0.6H_2O$	8.6	$Rb_{0.5}H_{1.5}Ti_4O_9{\cdot}0.6H_2O$	8.7
1/2	$KHTi_4O_9{\cdot}0.5H_2O$	9.0	$RbHTi_4O_9{\cdot}1.1H_2O$	9.3
3/4	$K_{1.5}H_{0.5}Ti_4O_9{\cdot}1.2H_2O$	9.8	$Rb_{1.5}H_{0.5}Ti_4O_9{\cdot}2.1H_2O$	11.3
1/1	$K_2Ti_4O_9{\cdot}2.2H_2O$	10.9		

[a] The values of d_{200} indicate the interlayer spacing.

Results and Discussion

Preparation Process. The synthetic process of the layer/tunnel hybrid titanate consists of two steps: (i) Tuning of the interlayer stoichiometry of the tetratitanate, i.e., x in the formula $M_xH_{2-x}Ti_4O_9{\cdot}nH_2O$ to be larger than 1. (Hereafter, M represents K and Rb ions unless otherwise specified.) (ii) Dehydration by gentle heating. The compositional modification in the first step was achieved by titrating the protonic tetratitanate $H_2Ti_4O_9{\cdot}1.2H_2O$ with a MCl/MOH aqueous solution. Table 1 summarizes the titrated products. The titration behavior is compatible with the cation-exchange processes reported previously.[17,20] For the range of x value greater than 1, three ion-exchanged tetratitanates (x = 1.0, 1.5, and 2.0) were isolated for K and two phases (x = 1.0 and 1.5) for Rb.

In the succeeding step, the K- or Rb-loaded tetratitanate $M_xH_{2-x}Ti_4O_9{\cdot}nH_2O$ of $x \geq 1$ was dehydrated thoroughly by prolonged heat treatment at 350 °C. The phase relationship for dehydrated products is summarized in Figure 2. The alkali/proton tetratitanate of $x \sim 1$ and ~ 2 yielded the octatitanate $M_2Ti_8O_{17}$ (phase I) and the tetratitanate $M_2Ti_4O_9$ (phase III), respectively, which agrees with the previous studies.[8,17] On the other hand, the material of $x \sim 1.5$ evolved a different single phase (phase II), the (200) spacing of which was composition dependent in the intermediate range between those for $M_2Ti_4O_9$ and $M_2Ti_8O_{17}$. Figure 3 shows the powder XRD patterns before and after the dehydration for the Rb material of typical stoichiometry of $x = 1.5$. A well-swollen layer structure of $Rb_{1.5}H_{0.5}$-

(12) Feist, T. P.; Mocarski, S. J.; Davies, P. K.; Jacobson, A. J.; Lewandowski, J. T. *Solid State Ionics* **1988**, *28–30*, 1338.
(13) Feist, T. P.; Davies, P. K. *J. Solid State Chem.* **1992**, *101*, 275.
(14) Sasaki, T.; Komatsu, Y.; Fujiki, Y. *Chem. Mater.* **1992**, *4*, 894.
(15) Rebbah, H.; Desgardin, G.; Raveau, B. *Mater. Res. Bull.* **1979**, *14*, 1125.
(16) Raveau, B. *Rev. Chim. Miner.* **1984**, *21*, 391.
(17) Sasaki, T.; Watanabe, M.; Komatsu, Y.; Fujiki, Y. *Inorg. Chem.* **1985**, *24*, 2265.
(18) Sasaki, T.; Watanabe, M.; Komatsu, Y.; Fujiki, Y. *Bull. Chem. Soc. Jpn.* **1985**, *58*, 3500.
(19) Sasaki, T.; Komatsu, Y.; Fujiki, Y. *Mater. Res. Bull.* **1987**, *22*, 1321.
(20) Sasaki, T.; Komatsu, Y.; Fujiki, Y. *Inorg. Chem.* **1989**, *28*, 2776.
(21) Sasaki, T.; Watanabe, M.; Fujiki, Y.; Kitami, Y. *J. Solid State Chem.* **1993**, *105*, 480.
(22) Fujiki, Y.; Ohta, N. *Yogyo Kyokaishi* **1980**, *88*, 111.
(23) Appleman, D. E.; Evans, H. T., Jr. Report No. PB216188, U.S. Department of Commerce, National Technical Information Service: Springfield, VA, 1973.

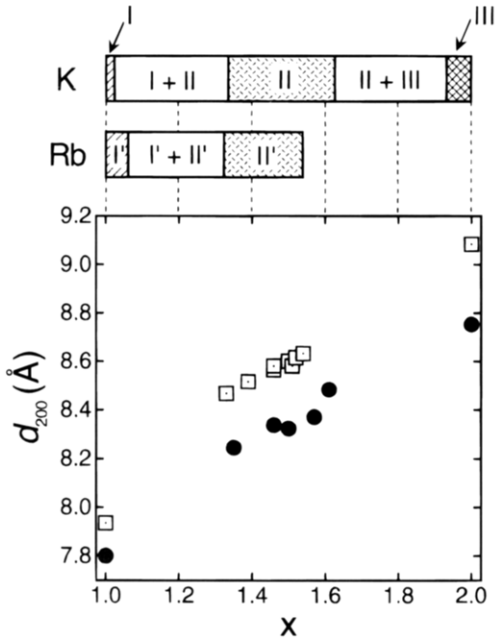

Figure 2. Dehydrated products and their (200) spacing as a function of the interlayer stoichiometry for the precursor tetratitanate. I, I': octatitanate $M_2Ti_8O_{17}$ (M = K, Rb). II, II': hybrid $M_{6+\delta}Ti_{16}O_{35+\delta/2}$. III: tetratitanate $K_2Ti_4O_9$. The value of x on the abscissa is for the chemical formula of $M_xH_{2-x}Ti_4O_9{\cdot}nH_2O$. The circles and squares represent the data for K and Rb, respectively. The (200) spacings at $x = 1.0$ and 2.0 are the values for $M_2Ti_8O_{17}$ and $M_2Ti_4O_9$, respectively.[8,10]

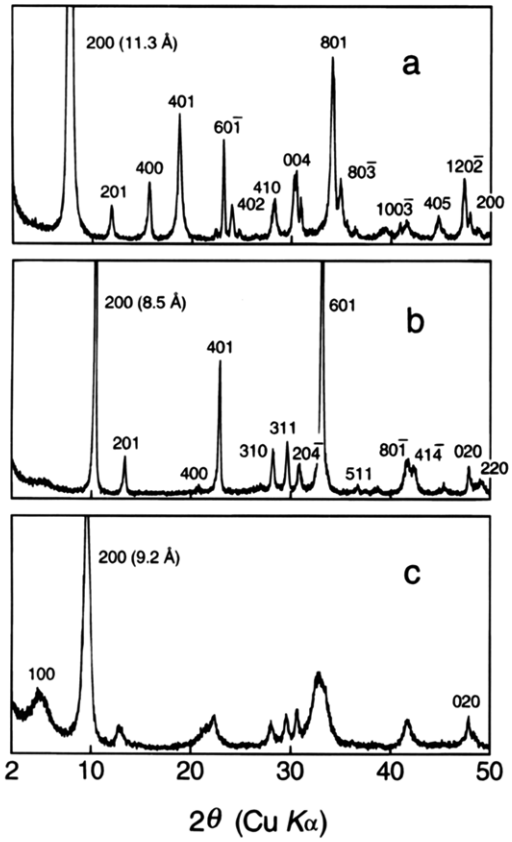

Figure 3. Powder XRD patterns of (a) $Rb_{1.5}H_{0.5}Ti_4O_9{\cdot}2.1H_2O$, (b) $Rb_6Ti_{16}O_{35}$, and (c) $Rb_6Ti_{16}O_{35}{\cdot}nH_2O$.

$Ti_4O_9{\cdot}2.1H_2O$ was collapsed. The (200) spacing, attributable to the separation of the titanate sheets, shrank appreciably by 2.8 Å. The K-phase also gave a similar pattern, evidently indicating isomorphous relationship to the Rb counterpart. Phase II is the intergrowth between $M_2Ti_4O_9$ and $M_2Ti_8O_{17}$, as will be presented in detail later. The general chemical formula is represented as $M_{6+\delta}Ti_{16}O_{35+\delta/2}$. The nonstoichiometric parameter δ ranges from -0.7 to $+0.5$. Another distinctive feature for phase II is its hygroscopic nature which is contrasting to $M_2Ti_8O_{17}$. The compound took up water by being immersed in aqueous solutions or even by being exposed to moist air. The spacing for the (200) line expanded on hydration (see Figure 3c) and reverted to the original value by heating at 300 °C. This phenomenon is attributable to the layer nature of phase II, at least in part, to be swollen.

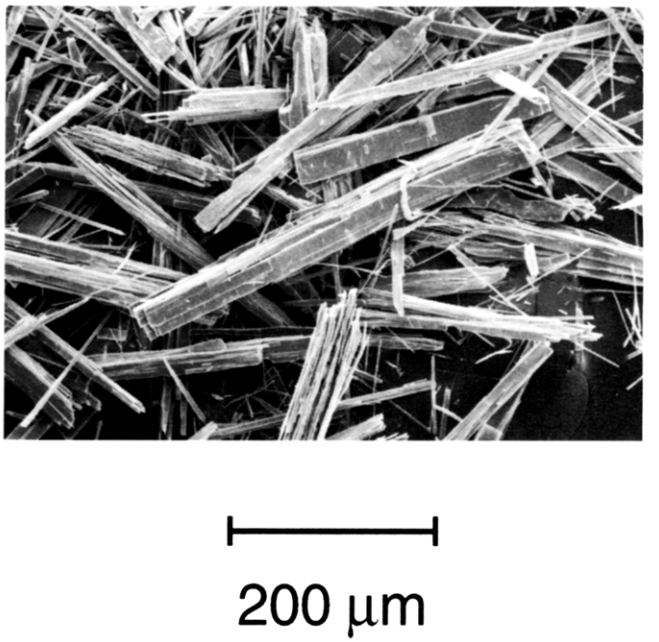

Figure 4. Scanning electron micrograph for $K_6Ti_{16}O_{35}$.

Table 2. Lattice Constants for the Layer/Tunnel Hybrid Titanate and Its Related Compounds

compound	a (Å)	b (Å)	c (Å)	β (deg)
$K_6Ti_{16}O_{35}$	16.581(7)	3.790(1)	11.956(6)	95.54(5)
$K_2Ti_4O_9$[a]	18.25(1)	3.791(1)	12.01(1)	106.4(1)
$K_2Ti_8O_{17}$[b]	15.678(2)	3.775(1)	11.951(1)	95.67(1)
$Rb_6Ti_{16}O_{35}$	17.144(7)	3.806(2)	11.953(7)	95.57(6)
$Rb_2Ti_4O_9$[a]	18.92(1)	3.797(5)	12.05(1)	106.2(1)
$Rb_2Ti_8O_{17}$[b]	15.961(3)	3.786(1)	11.918(2)	96.05(2)

[a,b] Quoted from refs 10 and 8, respectively.

The fibrous or needlelike morphology of the starting tetratitanate $K_2Ti_4O_9$ was preserved during the soft-chemical process as exemplified by the SEM photograph (Figure 4) for the final product $K_6Ti_{16}O_{35}$.

Diffraction Studies. The titanate $M_6Ti_{16}O_{35}$, the typical composition ($\delta = 0$) of phase II, was examined from a structural point of view. The powder XRD data can be indexed as a monoclinic lattice (see Figure 3), the refined parameters of which are listed in Table 2. The indexing suggests that the lattice type is primitive. Note that the related titanates, $M_2Ti_4O_9$ and $M_2Ti_8O_{17}$, have C-base-centered cells.

To get more conclusive information on the crystal symmetry, the reciprocal lattice of $Rb_6Ti_{16}O_{35}$ was examined by the electron diffraction technique. The Rb form was chosen because of its higher stability than its K counterpart, especially under electron beam irradiation in a transmission electron microscope. Figure 5

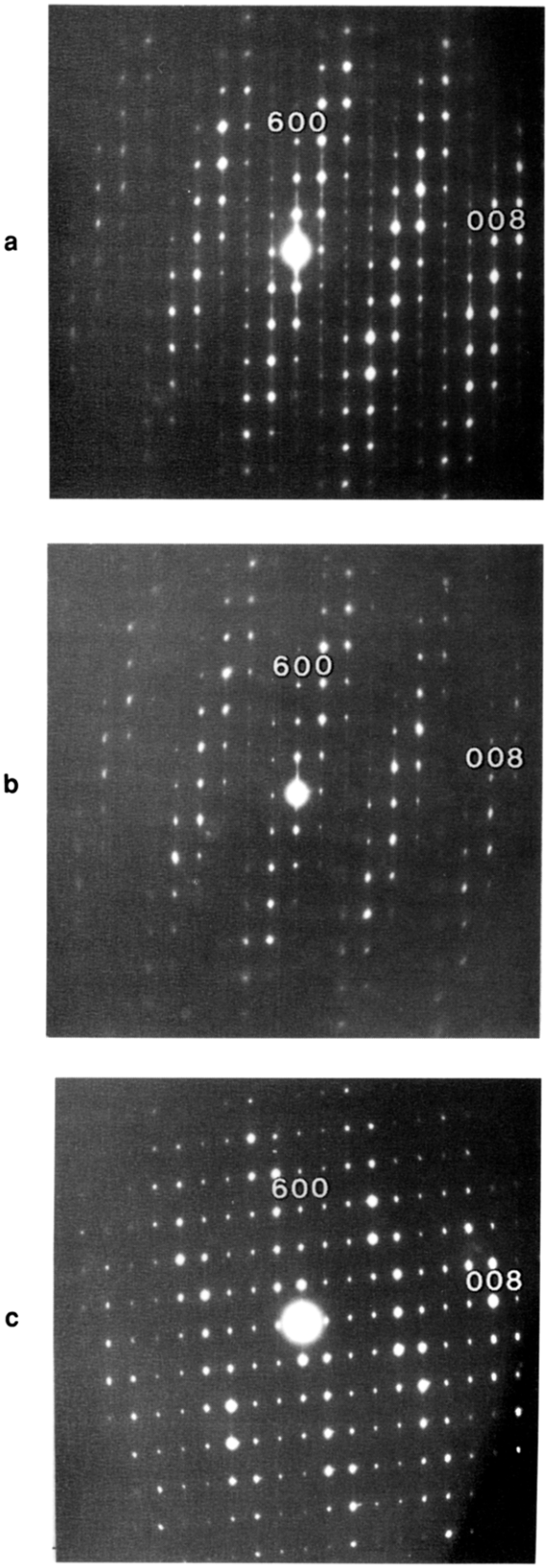

Figure 5. Electron diffraction patterns corresponding to the $h0l$ reciprocal lattice section for (a) $Rb_6Ti_{16}O_{35}{\cdot}nH_2O$, (b) $Rb_6Ti_{16}O_{35}$, and (c) $Rb_2Ti_8O_{17}$.

displays the $h0l$ reciprocal lattice section which is one of the most important for the structure. Two kinds of diffraction patterns were recognized: They were virtually similar except for slight discrepancies in cell parameters: $c^*/a^* \sim 1.4$ and $\beta \sim 93°$ for (a) while $c^*/a^* \sim 1.3$ and $\beta \sim 96°$ for (b). The difference may be associated with the hydration of $Rb_6Ti_{16}O_{35}$. The specimens were prepared by sectioning an acicular crystal (see Figure 4) in water with an ultramicrotome, which is likely to make some of the fragments hydrated. The coincidence of the β angle in (b) with the value refined from the XRD data (Table 2) as well as the smaller c^*/a^* ratio indicates that the pattern (b) is from an unhydrated form and the other from a hydrated one. Another evidence is based on the fact that the pattern (a) changed into (b) under an intense beam irradiation. The electron bombardment in a high-vacuum environment facilitates the evaporation of hydrated water.

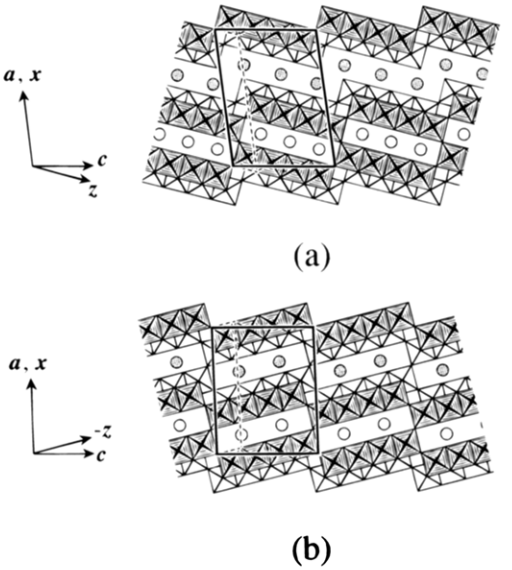

Figure 6. Polyhedral representation of the crystal structure for (a) $M_6Ti_{16}O_{35}$ and (b) $M_2Ti_8O_{17}$. Projection parallel to the b axis. The bold solid lines and dashed ones represent the unit cell and modulation pseudosubcell, respectively, and their axial systems are expressed by ($\boldsymbol{a}$, $\boldsymbol{c}$) and ($\boldsymbol{x}$, $\boldsymbol{z}$), respectively. Note that the drawings are in the right-hand system easy to compare to the reciprocal data shown in Figure 5.

The diffraction pattern was complex. On the $h00$ row, even reflections were bright while odd ones were faint and, in an extreme case, spread out along the a axis to become a rod. The intensity sequence of the $h00$ row was completely inverted on the $h04$ row (even, weak; odd, strong) and repeated again on the $h08$ row. The patterns in the intermediate region (the $h0l$ rows where $l = 1-3$ and $5-7$) were transient from the $h00$ to the $h04$, and from the $h04$ to the $h08$, respectively.

These distinctive diffraction features are summarized in comparison with the data for the related compound $Rb_2Ti_8O_{17}$ (Figure 5c) as follows: (i) The hybrid oxide $Rb_6Ti_{16}O_{35}$ revealed heavy diffuse streaks along the a^* while none were observed for $Rb_2Ti_8O_{17}$. (ii) The unit cell for $Rb_6Ti_{16}O_{35}$ is primitive while that for $Rb_2Ti_8O_{17}$ is C-base-centered.

The intensity distribution for the $h0l$ pattern of $Rb_6Ti_{16}O_{35}$ stands out with noticeable zones of enhanced diffraction spots running across in a slant direction. Similar enhancement was observed for $Rb_2Ti_8O_{17}$. This phenomenon suggests some modulation effect, the detailed analysis of which will be described later.

Structure Analysis. On the basis of the diffraction data above, the crystal structure of the hybrid titanate is derived as follows:

(i) The structure comprises the corrugated titanate sheet, stepped every four octahedra, which is also the primary structural component both for $M_2Ti_4O_9$ and M_2-

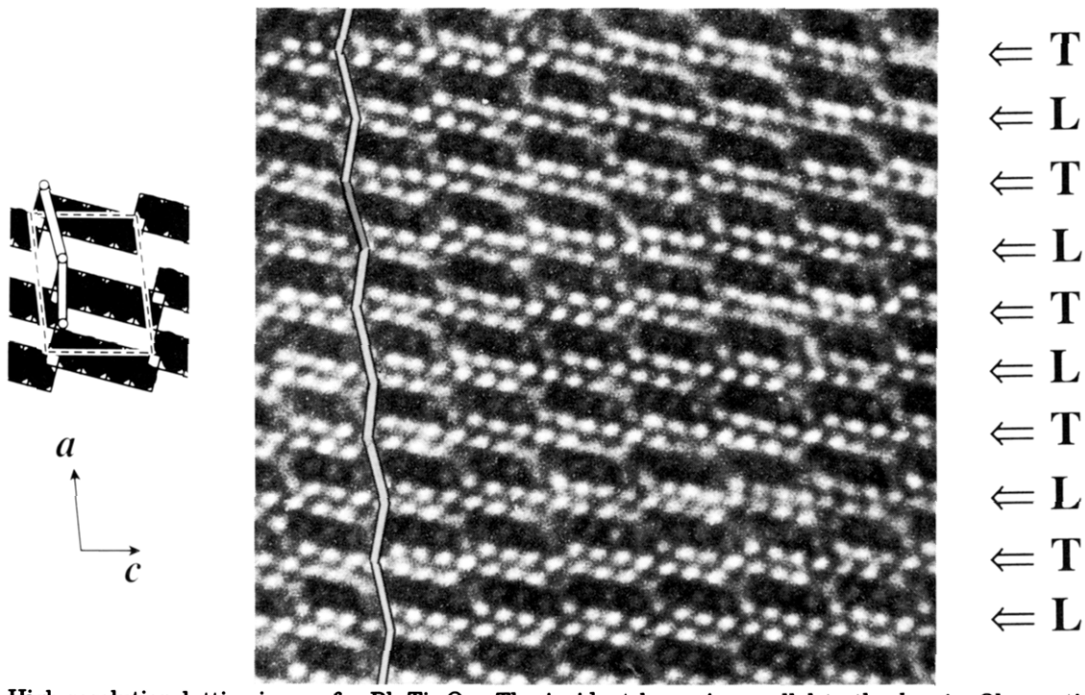

Figure 7. High-resolution lattice image for $Rb_6Ti_{16}O_{35}$. The incident beam is parallel to the *b* axis. Observation conditions: underfocus, ~380 Å; aperture, ~0.8 $Å^{-1}$ (~440 diffraction spots were enclosed.). Symbols L and T denote the layer structure part and the tunnel one, respectively.

Ti_8O_{17}. This is from the fact that dimensions for the *b* and *c* axes are almost equal to those in $M_2Ti_4O_9$ and $M_2Ti_8O_{17}$ as seen in Table 2.

(ii) A primitive unit cell, the (200) spacing (=(*a*/2) sin β) of which is close to the mean of the corresponding values for $M_2Ti_4O_9$ and $M_2Ti_8O_{17}$, is accounted for by an intergrowth between the tetratitanate-type layer unit of $Ti_8O_{18}^{4-}$ and the octatitanate-type tunnel one of $Ti_8O_{17}^{2-}$, which is consistent with the suggestion by Tournoux et al.[3,6,7] The idealized polyhedral drawing of the structure is shown in Figure 6a. The diffuse streaks along the a^* implies that the layer/tunnel sequence is not perfectly ordered.

Straightforward evidence for the hybrid structure was provided by a (010) high-resolution lattice image (see Figure 7) from a transverse-sectioned crystal fragment of $Rb_6Ti_{16}O_{35}$. The observed contrast makes good matching to the structure derived. The dark block corresponds to the vertical projection of corrugated titanate ribbons of four octahedra wide and the dark spot in the interstices is assignable to Rb ions. It is inconclusive to identify the intergrowth by the small ~1 Å difference in thickness for the layer structure unit and the tunnel one.[24] On the other hand, the intergrowth was discerned unambiguously from the difference in lateral displacement of the titanate blocks, parallel to the *z* axis in Figure 6a, between the layer part and the tunnel region. The titanate blocks are stacked along the *a* axis in a staggered manner as emphasized by the zigzag line in the image. The blocks are displaced with respect to one another by ~4.5 Å (corresponding to approximately one and a half octahedron dimension) in the layer part while ~1.5 Å in the tunnel region. This is consistent with the structure in Figure 6a. A comparable plot gives a straight line both for the pure layer structure of $M_2Ti_4O_9$ and the tunnel one of $M_2Ti_8O_{17}$.[11]

Raveau and his collaborators have studied intergrowth phenomena of oxides, some of which show similarities, in some respects, to the hybrid titanate $M_6Ti_{16}O_{35}$ presented here. One example is the oxide $K_4Ti_{10}Nb_2O_{27}$ which is prepared from the layered material $H_3Ti_5NbO_{14}\cdot H_2O$ through an analogous process to that for $M_6Ti_{16}O_{35}$, namely, ion-exchange and dehydration.[25] The proposed structural model for $K_4Ti_{10}Nb_2O_{27}$ is also very similar to $M_6Ti_{16}O_{35}$, being characterized by a layer/tunnel hybrid: an intergrowth of hexatitanate ($K_2Ti_6O_{13}$)-type tunnel and trititanate ($Na_2Ti_3O_7$)-type layer. Only difference is the lateral dimension of basic structural units of the host frameworks; three octahedra wide for $K_4Ti_{10}Nb_2O_{27}$ and four for $M_6Ti_{16}O_{35}$.

Another related titanate is $M_4M'Ti_{16}O_{35}$ (M, alkali metal; M′, alkaline earth metal).[26,27] The composition of its host lattice is identical to that of the hybrid oxide. The titanate is a member of a structural series in which two kinds of tunnel structures; hexatitanate $M_2Ti_6O_{13}$ and hypothetical tetratitanate $M'Ti_4O_9$, are intergrown along the *c* axis. The 2/1 intergrowth gives $M_4M'Ti_{16}O_{35}$. The intergrowth of $M_2Ti_6O_{13}/M'Ti_4O_9$ may be thermodynamically stable, being prepared at high temperatures above 1200 °C. In contrast, the hybrid material, the layer/tunnel intergrowth along the *a* axis, is metastable as will be addressed below and is obtained only through the soft-chemical process presented here.

Interpretation of the Modulation Effect. As pointed out above, the *h0l* reciprocal lattice section, both for $Rb_6Ti_{16}O_{35}$ and $Rb_2Ti_8O_{17}$, revealed characteristic zones of enhanced diffraction spots. This noticeable

(24) The thickness of the layer structure for $Rb_2Ti_4O_9$ is 9.07 Å[10] (corresponding to the (200) spacing) and that of the tunnel for $Rb_2Ti_8O_{17}$ is 7.94 Å.[8]

(25) Grandin, A.; Borel, M. M.; Hervieu, M.; Raveau, B. *J. Solid State Chem.* **1987**, *68*, 369.

(26) Hervieu, M.; Desgardin, G.; Raveau, B. *J. Solid State Chem.* **1979**, *30*, 375.

(27) Hervieu, M.; Desgardin, G.; Raveau, B. *Phys. Status Solidi* **1980**, *60*, 237.

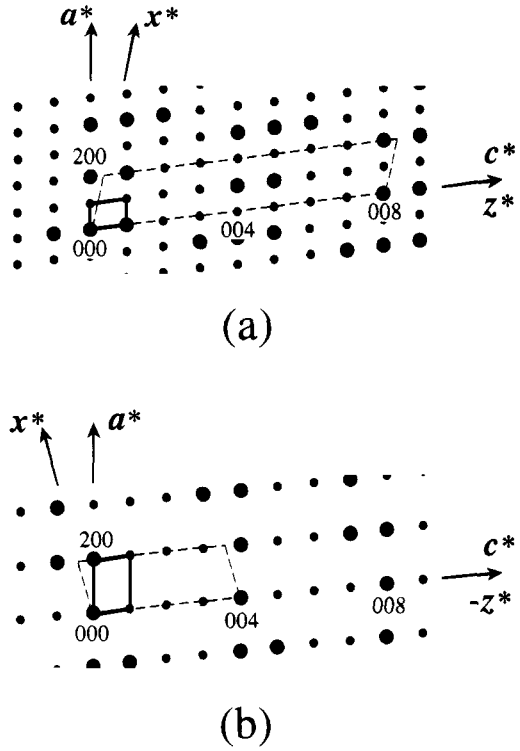

Figure 8. Idealized representation of the $h0l$ reciprocal lattice section for (a) $Rb_6Ti_{16}O_{35}$ and (b) $Rb_2Ti_8O_{17}$. The axial notation is identical to that in Figure 6.

Table 3. Crystallographic Data Derived from Electron Diffraction Data

	$Rb_6Ti_{16}O_{35}$	$Rb_2Ti_8O_{17}$
basic unit cell	primitive	C-base-centered
	$a \sim 17$ Å	$a \sim 16$ Å
	$b \sim 3.8$ Å	$b \sim 3.8$ Å
	$c \sim 12$ Å	$c \sim 12$ Å
	$\beta \sim 97°$	$\beta \sim 96°$
modulation pseudosubcell	body-centered	C-base-centered
	$x(a) \sim 16$ Å	$x(a) \sim 16$ Å
	$y(b) \sim 3.8$ Å	$y(b) \sim 3.8$ Å
	$z \sim 3$ Å	$z \sim 3$ Å
	$\beta' \sim 108°$	$\beta' \sim 100°$

feature is explained by superimposition of two lattices with different cell parameters, namely, "coincidence-site lattice".[28,29] One is the unit cell and the other is a modulation periodicity.

The geometry of the basic unit cell and the overlying modulation pseudosubcell is schematically illustrated in Figure 8 and their parameters are tabulated in Table 3. Note the differences between $Rb_6Ti_{16}O_{35}$ and $Rb_2Ti_8O_{17}$ in symmetry of the pseudosubcell as well as inclination of the x^* axis with respect to the a^*. The face-centered arrangement of the enhanced spots was definitely observed for $Rb_6Ti_{16}O_{35}$. A similar relationship was also recognized in the $0kl$ pattern, which indicates that the modulation pseudocell is body-centered in the real space. The comparable subcell for $Rb_2Ti_8O_{17}$ is C-base-centered.

These modulation effects can be understood on the basis of the crystal structures for $Rb_6Ti_{16}O_{35}$ and $Rb_2Ti_8O_{17}$. The unit cells for both structures include distinguishing structural subunits based on TiO_6 octahedra as enclosed by dashed lines in Figure 6. The geometrical relationships between the unit cell and the subunit are compatible with those observed in the reciprocal space (Figure 8). Furthermore, the subunit for each structure satisfies the requirements for the symmetry deduced from the electron diffraction data. A body-centered configuration is actually the case in $Rb_6Ti_{16}O_{35}$ except for a slight deviation from it and a C-base-centered relationship is essentially fulfilled in $Rb_2Ti_8O_{17}$. The overall view of the arrangement of the subunits is illustrated in Figure 9. The repetition of the subunits is substantially infinite along the $x(a)$ axis but only four parallel to the z, making a macromolecule-like slab. The slabs are arranged leaving some space between them, the magnitude of which is incommensurate to the periodicity of the subunits. Hence the whole diffraction from the system can be considered as convolution of inter- and intraslab interferences. The short range of coherency for the latter as well as small distortions and differences in contents of the subunit makes the diffraction from the subunit spread along the z^* axis, which was visible by the broad zones of enhancement.

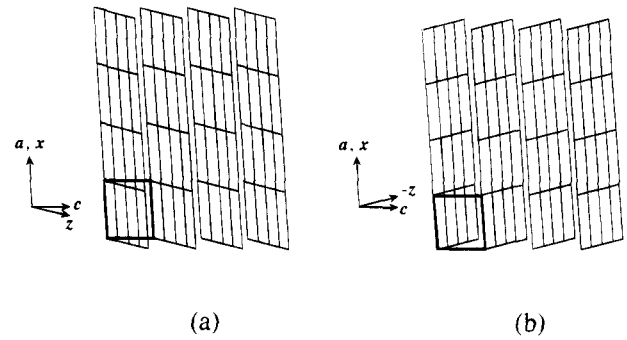

Figure 9. Arrangements of the structural subunits for (a) $M_6Ti_{16}O_{35}$ and (b) $M_2Ti_8O_{17}$. The unit cell and the subunit are indicated by bold and thin lines, respectively. The axial notation is identical to that in Figure 6.

Similar diffraction phenomena have been encountered in crystallographic shear (CS) structures.[30] One of the well-known examples is the Magneli phases, a homologous series of oxygen-deficient oxides derived from rutile structure by introducing CS planes. The unit cell and the subunit in $Rb_6Ti_{16}O_{35}$ are comparable to the ordered CS and the sublattice of rutile, respectively. The diffraction of $Rb_6Ti_{16}O_{35}$ may be parallel to that for a heavily reduced member of the Magneli phases in which CS planes recur at a short interval.

There are a variety of alkali titanates, including three kinds of oxides described here, the general formula of which is represented as $A_2Ti_nO_{2n+1}$ (A, alkali metals; $n = 3-8$).[31-34] They are characterized by a layered or tunnel structure which is built up from corrugated ribbons of edge-sharing three-to-five TiO_6 octahedra. Structural subunits, analogous to those in $Rb_6Ti_{16}O_{35}$ and $Rb_2Ti_8O_{17}$, can be extracted from these structures and therefore a similar modulation effect is expected.

(28) Bollmann, W. *Crystal Defects and Crystalline Interfaces*; Springer-Verlag: Berlin, 1970.
(29) Bollmann, W. *Surf. Sci.* **1972**, *31*, 1.
(30) Anderson, J. S. *Intercalation Chemistry*; Whittingham, M. S., Jacobson, A. J., Eds.; Academic Press: New York, 1982.
(31) Andersson, S.; Wadsley, A. D. *Acta Crystallogr.* **1961**, *14*, 1245.
(32) Andersson, S.; Wadsley, A. D. *Acta Crystallogr.* **1962**, *15*, 194.
(33) Wadsley, A. D.; Mumme, W. G. *Acta Crystallogr.* **1968**, *B24*, 392.
(34) Grey, I. E.; Madsen, I. C.; Watts, J. A.; Bursill, L. A.; Kwiatkowska, J. *J. Solid State Chem.* **1985**, *58*, 350.

Actually triple or quintuple multiplicity of a particular axis has been pointed out in the electron diffraction patterns for $Na_2Ti_3O_7$ and $Cs_2Ti_5O_{11}$,[13,35] but no explanation has been given. These could be interpreted in an analogous manner to the analysis described here.

Formation Scheme. The close structural relationship between the hybrid oxide $M_6Ti_{16}O_{35}$ and its precursor tetratitanate $K_2Ti_4O_9$ readily provides insight on its filiation scheme: Half of the host layers in $K_2Ti_4O_9$ are joined in a topotactic fashion while the other half are left open. The alkali/proton tetratitanate, $M_{1.5}H_{0.5}Ti_4O_9{\cdot}nH_2O$, accommodates three cations and one proton, besides hydrated water, in the unit interlayer space. On heating, interlayer water molecules were evaporated first, which was completed up to 150 °C.

After all the interlayer water molecules leave the lattice, namely, in $M_{1.5}H_{0.5}Ti_4O_9$, a persisting proton is bound to unshared corner oxygen atoms designated by closed squares in Figure 1a. This oxygen atom is the most basic in the host framework, as has been discussed experimentally as well as theoretically.[3,17,36] Further heating above 150 °C splits out water from a pair of facing hydroxyl groups on adjacent host layers so as to make them linked. It is worth noting that only half of the terminal oxygen atoms bear protons in $M_{1.5}H_{0.5}Ti_4O_9$. Therefore, the migration of half of the protons from one side of the host layer to its other side is prerequisite to promote condensation, which takes place ideally in every second interlayer space to produce the layer/tunnel hybrid structure. Small windows indicated in Figure 1a may offer the path for the protons. On the other hand, similar migration may be unlikely for K and Rb ions because of their larger size. As a consequence, the cation distribution shown in Figure 7, half three in the interlayer space and the other half in the tunnel, is most likely.

The wide range of nonstoichiometry, $-0.7 < \delta < 0.5$ in $M_{6+\delta}Ti_{16}O_{35+\delta/2}$, is tolerated by variation in the layer/tunnel ratio, $(1/2 + \delta/4)/(1/2 - \delta/4)$. The layer/tunnel proportion is changeable from 36/64 to 62/38, along which the (200) spacing increased continuously as shown in Figure 2, and is determined by the interlayer stoichiometry of the intermediate alkali/proton tetratitanate. It is to be pointed out that the 3/4-cation loaded phase possessed a fairly wide range of miscibility around their specific stoichiometry ($x = 1.5$), which is the origin of the nonstoichiometric nature of the hybrid oxide. A poor alkali content ($x < 1.5$) means a larger number of hydroxyl groups, which in turn makes more host layers be connected and vice versa.

The total intergrowth from the pure octatitanate structure to the tetratitanate one, that is to say, over the full range of x in Figure 2, was not observed in the present study, being in conflict with the results of Tournoux et al.[3,6,7] The two immiscible phases were present in the loading range of $1.1 < x < 1.3$ and $1.6 < x < 1.9$. One was the hybrid oxide and the other was $M_2Ti_8O_{17}$ or $M_2Ti_4O_9$, respectively. The phase relationship is an exact reflection of that of the precursor, or the alkali/proton tetratitanate $M_xH_{2-x}Ti_4O_9{\cdot}nH_2O$. As presented in Table 1, discontinuous phase transformations took place successively when the protonic tetratitanate $H_2Ti_4O_9{\cdot}1.2H_2O$ was titrated with alkali metal ions. Two cation-exchanged phases, one is of a lower loading and the other of a higher conversion, coexisted in the loading range of x above, which were converted into two discrete dehydrated products.

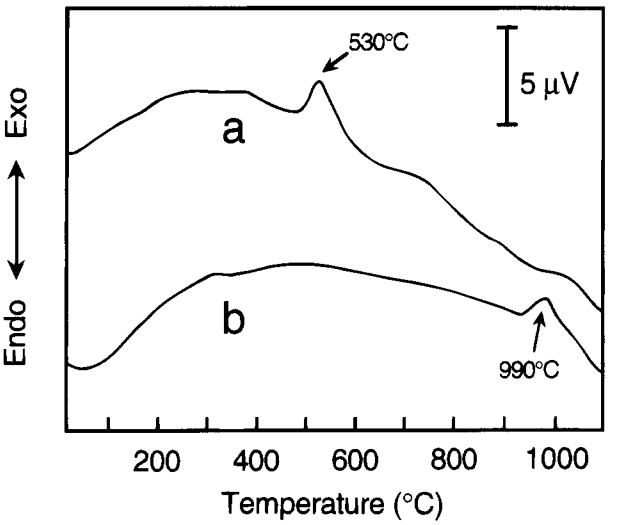

Figure 10. Differential thermal analysis curves for (a) $K_6Ti_{16}O_{35}$ and (b) $Rb_6Ti_{16}O_{35}$. Heating rate: 10 °C min^{-1}.

The starting tetratitanate $K_2Ti_4O_9$ in this laboratory was flux-grown probably having a higher degree of crystallinity than that in Tournoux's which was prepared by simple calcination. The miscibility range for the 3/4-loaded phase may be widened for a less crystalline sample and eventually a continuous solid solution may form in the entire course of the cation-exchange process. In such a case, the whole intergrowth could occur although the material may not be well-defined. Similar cation-exchange properties have been reported for α-zirconium phosphate which can be synthesized in various degrees of crystallinity.[37]

Thermal Stability. The hybrid oxide $M_6Ti_{16}O_{35}$ was decomposed at elevated temperatures. The differential thermal analysis curve (see Figure 10) exhibited an exothermic peak at 530 and at 990 °C for $K_6Ti_{16}O_{35}$ and $Rb_6Ti_{16}O_{35}$, respectively, where the hybrid oxide was disproportionated into a mixed phase of $M_2Ti_6O_{13}$ and $M_2Ti_4O_9$.

The stability of ionic crystals is strongly influenced by the degree of local charge neutrality. Pauling's electrostatic valence rule[38] is successfully applied to discuss the stability of a class of alkali titanates $A_2Ti_nO_{2n+1}$ (A, alkali metals; $n = 4-8$), in which alkali metal ions, N_A in number, are distributed over distorted cubic sites, N_C in number, where $N_A < N_C$. The survey on the titanates suggests that the cation occupation of over two thirds of the cubic sites ($N_A/N_C > 2/3$) is required to stabilize the structure, at least, in a high temperature region. The host framework of $M_6Ti_{16}O_{35}$ supplies five cubic sites in the unit interlayer region and four in the unit tunnel. Accommodation of three K or Rb ions in the tunnel part ($N_A/N_C = 3/4$) is higher than the threshold, being adequate to attain sufficient charge neutrality. The octatitanates with the same cation

(35) Bursill, L. A.; Smith, D. J.; Kwiatkowska, J. *J. Solid State Chem.* **1987**, *69*, 360.
(36) Dronskowski, R. *J. Am. Chem. Soc.* **1992**, *114*, 7230.
(37) Clearfield, A. *Inorganic Ion Exchange Materials*; CRC Press: Boca Raton, FL, 1982.
(38) Pauling, L. *The Nature of the Chemical Bond*, 3rd ed.; Cornell University Press: Ithaca, NY, 1960.

Table 4. Elution of K Ions by an Acid Leaching[a]

compound	elution (%)	structure
$K_6Ti_{16}O_{35}$	48	layer/tunnel
$K_2Ti_8O_{17}$	2	tunnel
$K_2Ti_4O_9$	100	layer
$K_{1.5}H_{0.5}Ti_4O_9 \cdot 1.2H_2O$	98	layer

[a] Solid: 0.1 g. Acid: 0.2 mol dm^{-3} HCl solution, 20 cm^3. Temperature: 80 °C.

content ($N_A/N_C = {}^3/_4$), e.g., bronzelike $K_3Ti_8O_{17}$[8,39] and its isomorphous compounds such as $K_3AlTi_7O_{17}$,[40] are stable at high temperatures (~1000 °C) while its analog $M_2Ti_8O_{17}$ having only two cations in the tunnel ($N_A/N_C = {}^2/_4$) is metastable.[8] On the contrary, the cation population in the layer structure part ($N_A/N_C = {}^3/_5$) may be too sparse to achieve the local charge neutrality. Tetratitanate $K_2Ti_4O_9$, which may be thermodynamically stable, contains four cations in a comparable space ($N_A/N_C = {}^4/_5$).

Cation Exchange. The hybrid oxide $M_6Ti_{16}O_{35}$ eluted approximately a half of the constituent alkali metal ions by being leached in acid solutions (see Table 4). Similar acid treatments extracted nearly 100% of the cations from the layered structure of $M_2Ti_4O_9$ while a negligible amount of the cations was removed from the tunnel oxide $M_2Ti_8O_{17}$ (Table 4). The leaching characteristics of these three kinds of oxides substantiate the foregoing discussion on the cation distribution in $M_6Ti_{16}O_{35}$. The half of the cations, which are located in the interlayer region, are responsible for the ion-exchange reaction, while the other half, confined in the tunnel, are not accessible:

$$K_6Ti_{16}O_{35}(s) + 3H^+(aq) + 3H_2O(aq) \rightarrow \underset{[8.3\ \text{Å}]}{} \underset{}{} H_3K_3Ti_{16}O_{35}\cdot 3H_2O(s) + 3K^+(aq) \quad (1)$$
$$\underset{[8.5\ \text{Å}]}{}$$

where numerals in parentheses denote the (200) spacing.

The resulting protonated material took up K ions on the action of a KOH solution, reversibly reproducing the original hybrid compound (hydrated form).

Reductive Intercalation. The hybrid titanate $M_6Ti_{16}O_{35}$ spontaneously undergoes reductive K and Li intercalation by being interacted with K metal vapor and with n-C_4H_9Li, respectively:

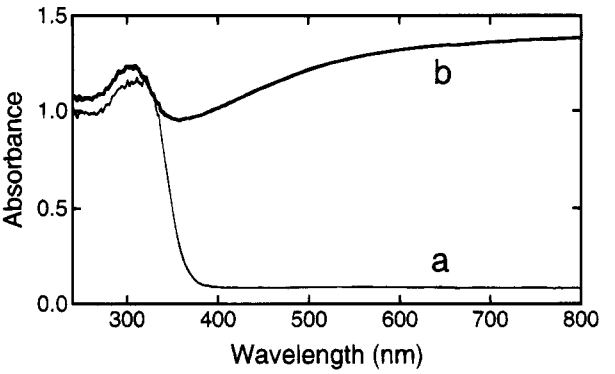

Figure 11. Reflectance spectra for (a) $K_6Ti_{16}O_{35}$ and (b) $K_{1.5}K_6Ti_{16}O_{35}$.

Table 5. Compositions and Lattice Constants for the Chemically Reduced Hybrid Titanates

compound	a (Å)	b (Å)	c (Å)	β (deg)
$K_{1.5}K_6Ti_{16}O_{35}$	16.48(2)	3.825(3)	12.086(9)	97.12(6)
$Li_{1.2}K_6Ti_{16}O_{35}$	16.48(1)	3.797(1)	11.985(6)	95.06(7)
$K_{2.9}Rb_{4.5}Ti_{16}O_{35}$	16.96(2)	3.811(5)	11.94(1)	96.7(1)
$Li_{1.1}Rb_6Ti_{16}O_{35}$	17.115(4)	3.810(1)	12.019(5)	95.59(3)

$$M_6Ti_{16}^{IV}O_{35} + xA \rightarrow A_xM_6Ti_x^{III}Ti_{16-x}^{IV}O_{35} \quad (2)$$

where A = Li, K. The reaction was completed within 3 days which can be monitored by its color change to bluish-black (see Figure 11) characteristic for mixed valent titanates. The K uptake per formula weight, or x in the above equation, was ~1.5. The composition for the Rb material suggests simultaneous cation-exchange accompanied by reduction. The degree of Li intercalation ranged from 0.5 to 1.2, which was dependent on the dose of the reductant. The hybrid structure was not destroyed on reduction, which is suggested from the lattice parameter refinements (Table 5). A small but significant shrinkage in a axis and a contrasting expansion in b clearly shows that the cations were incorporated into the lattice. The former change may be accounted for by the increment of Coulombic attraction between the host framework and the guest cations, and the latter by increased repulsion between the cations.

The additional cations are presumably incorporated in the interlayer space since the material has a room, the dimension of which is capable of accommodating one cation or more per chemical formula. This is roughly in harmony with the observed composition of the products.

Acknowledgment. The authors thank Mr. S. Takenouchi, National Institute for Research in Inorganic Materials, for his contribution in chemical analyses.

(39) Watts, J. A. *J. Solid State Chem.* **1970**, *1*, 319.
(40) Patarin, J.; Marchand, R.; Tournoux, M. *Ann. Chim. Fr.* **1985**, *10*, 139.